

Article

# Spatiotemporal Assessment of Irrigation Performance of the Kou Valley Irrigation Scheme in Burkina Faso Using Satellite Remote Sensing-Derived Indicators

Alidou Sawadogo<sup>1,\*</sup>, Louis Kouadio<sup>2</sup> , Farid Traoré<sup>3</sup> , Sander J. Zwart<sup>4</sup> , Tim Hessels<sup>5</sup>  
and Kemal Sulhi Gündoğdu<sup>1</sup>

<sup>1</sup> Biosystems Engineering Department, Faculty of Agriculture, University of Uludag, Görükle Kampüsü, Nilüfer, Bursa 16059, Turkey; kemalg@uludag.edu.tr

<sup>2</sup> Center for Applied Climate Sciences, University of Southern Queensland, West Street, Toowoomba, QLD 4350, Australia; louis.kouadio@usq.edu.au

<sup>3</sup> Institut de l'Environnement et de Recherches Agricoles, Guisga Street, Ouagadougou, P.O. Box 8645 Ouagadougou 04, Burkina Faso; farid.traore@yahoo.fr

<sup>4</sup> International Water Management Institute (IWMI), Cantonments, Accra, PMB CT 112, Ghana; s.zwart@cgiar.org

<sup>5</sup> Department of Water Management, Delft University of Technology, Postbus 5, 2600 AA Delft, The Netherlands; timhessels@hotmail.com

\* Correspondence: alidousawadogo@uludag.edu.tr; Tel.: +905317614750

Received: 12 July 2020; Accepted: 3 August 2020; Published: 11 August 2020



**Abstract:** Traditional methods based on field campaigns are generally used to assess the performance of irrigation schemes in Burkina Faso, resulting in labor-intensive, time-consuming, and costly processes. Despite their extensive application for such performance assessment, remote sensing (RS)-based approaches remain very much underutilized in Burkina Faso. Using multi-temporal Landsat images within the Python module for the Surface Energy Balance Algorithm for Land model, we investigated the spatiotemporal performance patterns of the Kou Valley irrigation scheme (KVIS) during two consecutive cropping seasons. Four performance indicators (depleted fraction, relative evapotranspiration, uniformity of water consumption, and crop water productivity) for rice, maize, and sweet potato were calculated and compared against standard values. Overall, the performance of the KVIS varied depending on year, crop, and the crop's geographical position in the irrigation scheme. A gradient of spatially varied relative evapotranspiration was observed across the scheme, with the uniformity of water consumption being fair to good. Although rice was the most cultivated, a shift to more sweet potato farming could be adopted to benefit more from irrigation, given the relatively good performance achieved by this crop. Our findings ascertain the potential of such RS-based cost-effective methodologies to serve as basis for improved irrigation water management in decision support tools.

**Keywords:** water management; food security; climate variability; SEBAL; sub-Saharan Africa

## 1. Introduction

Water resources for irrigation are increasingly becoming scarce in many parts of the world due to a rapidly growing world population, pressure on water resources, and competing demands from other sectors (industrial and domestic sectors) [1–4]. In many countries, particularly in sub-Saharan African countries, irrigated agriculture is critical to the national economy, food security, and the livelihoods of local communities [5–7]. In Burkina Faso, the development of hydro-agricultural areas, consisting of small to medium water reservoirs and irrigated schemes, to cope with the impacts

of year-to-year rainfall variability on crop production has put substantial pressure on available water for irrigation [8,9]. The need for a more efficient use of water resources has become a paramount concern for the sustainability of agricultural production.

The performance assessment of irrigation schemes has been an integral part of water management to set benchmarks, improve system operations, assess the impacts of interventions and constraints, and assess progress towards strategic goals [10,11]. Such assessments are conducted by defining and quantifying key indicators and analyzing progress towards the goals [12,13]. Data requirements, however, are high and data are rarely collected or are unreliable or not readily accessible [10,14]. These data include meteorological data (e.g., rainfall, actual and potential evapotranspiration), discharge measurements, crop information (e.g., cultural coefficients, crop water requirements, biomass growth), topography, and soil data. In countries such as Burkina Faso, traditional methods based on field campaigns and surveys are generally used to assess the performance of irrigation schemes, making the process labor-intensive, time-consuming, and often expensive [7,15–17]. To make performance assessment more time and cost efficient, novel techniques and approaches are required. Satellite remote sensing (RS)-based approaches have been explored as cost-effective alternatives (see reviews in [14,18,19]). In general, RS can provide spatially explicit and objective information across different spatial (ranging from individual fields to watersheds) and temporal scales [14]. With the ongoing developments in RS data processing capacity and the availability of high temporal (real-time imagery) and spatial resolution data, RS-based approaches for assessing irrigation performance are more than crucial in data-scarce regions or countries such as Burkina Faso.

Several studies have been carried out to assess the performance of irrigation schemes under various environmental and management conditions using RS-based approaches (for examples, see [20–25]). For instance, Ref. [20] used RS data from the National Oceanic and Atmospheric Administration–Advanced Very High Resolution Radiometer (NOAA-AVHRR), complemented with in situ measurements, to monitor the performance of the Nilo Coelho scheme (which includes perennial fruit tree irrigation) in Brazil. In [21], researchers proposed an approach based on remote sensing data at a high level of spatio-temporal detail (i.e., Landsat-5 and Landsat-7 normalized difference vegetation index (NDVI) data and solar radiation data derived from the land surface analysis satellite applications facility) to assess the performance of a 800-km<sup>2</sup> rice-based irrigation system in Mali. Despite the extensive application of RS-based approaches for investigating the performance of irrigation schemes and guiding irrigation water management, such methodologies remain very much underutilized operationally in Burkina Faso. For instance, Refs. [16,17] used field monitoring and survey data to assess the performance of irrigated agricultural areas for paddy rice farming across the Kou Valley irrigation scheme (KVIS) during the early 2000s (in the former study) and for green bean, maize, and onion farming around two Burkinabe water reservoirs, the Savili and Mogtédó reservoirs (in the latter study). Both studies emphasized the necessity of better knowledge of the evolution of performance levels for timely and effective remedial actions.

The aim of this study was to assess the irrigation performance of the KVIS using satellite remote sensing-derived indicators. This study will focus on diagnostic performance indicators with the purpose of detecting areas with good and poor performance across the KVIS. The Python module for the Surface Energy Balance Algorithm for Land model (PySEBAL) was applied to fourteen high-resolution Landsat images obtained during the dry season production periods in 2013 and 2014 to estimate the actual evapotranspiration (ET<sub>a</sub>) and biomass at different temporal scales. Before proceeding with the calculations of performance indicators and subsequent analyses, we assessed the quality of the estimated PySEBAL-ET<sub>a</sub> values by comparing those from the Food and Agricultural Organization of the United Nations Water Productivity Open-access portal (FAO-WaPOR). Estimated PySEBAL-ET<sub>a</sub> and biomass were then used to analyze four performance indicators (i.e., the relative evapotranspiration, depleted fraction, uniformity of water consumption, and crop water productivity) for rice (*Oryza glaberrima*), maize (*Zea mays* L.), and sweet potato (*Ipomoea batatas*). The findings of this study could provide

valuable insights for guiding agricultural advisory services for the KVIS and ascertain the potential use of such a cost-effective approach for improving irrigation water management in Burkina Faso.

## 2. Materials and Methods

### 2.1. Study Area

Built in 1973, the KVIS is a 1200-ha irrigation scheme divided into eight blocks (Figure 1A) and is characterized by a diversity of crops, including cereals, tubers, and vegetables. The KVIS is located in the Kou watershed in southwest Burkina Faso. The Kou watershed is relatively rich in water resources due to several perennial water sources (Figure S1) [3,16]. It is characterized by a sub-humid climate [26,27] with two main climatic seasons: a rainy season from June to September followed by a dry season from October to May [27]. Monthly temperatures vary between 18 °C and 37 °C on average, and relative humidity values range from 20 to 80% depending on the season [27]. The average annual rainfall varies between 900 and 1100 mm, with an annual potential evapotranspiration of 2000 mm on average [16,28].

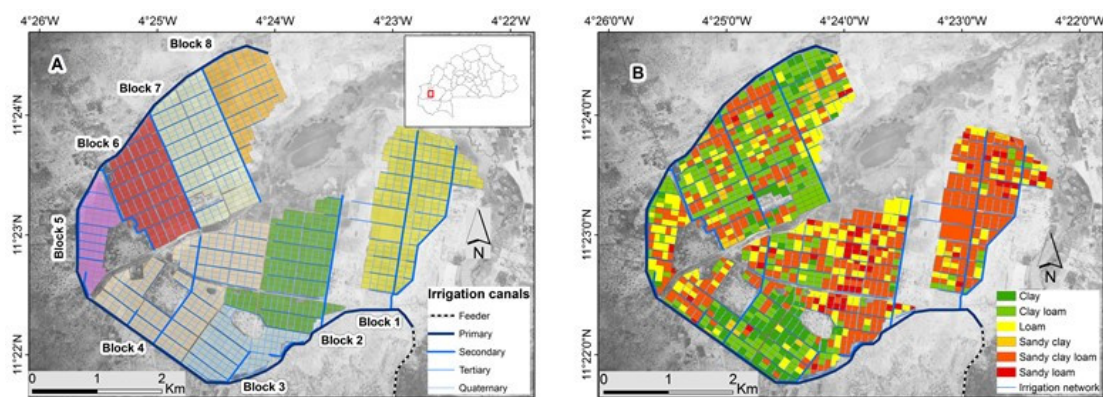


**Figure 1.** Distribution of irrigation canals and blocks (A) and dominant soil types per plot (B) at the Kou Valley irrigation scheme, Burkina Faso. Adapted from [29].

The Kou River and its tributaries drain the watershed area. From the headwork, water is gravitationally conveyed through a feeder canal at flow rates of 1.4 and 3.5 m<sup>3</sup> s<sup>-1</sup> on average during the dry and rainy seasons, respectively [3]. A hierarchical irrigation canal system from primary to quaternary canals allocates water across the scheme area (Figure 1A).

Six dominant soil types are found across the KVIS [16,29]: clay, clay loam, sandy clay, sandy clay loam, loam, and sandy loam (Figure 1B). More than 1300 farmers are reported to work at the KVIS (as of 2018; pers. comm. Lassané Kaboré). Individual farmer plot sizes vary between 0.2 and 1.5 ha, with gravity-fed surface irrigation being practiced across the scheme.

The KVIS has seen its performance decline over recent decades due to a combination of unfavorable weather conditions, a lack of maintenance of hydraulic infrastructures, poor agronomic management, and organizational failure [16,29–31]. Indeed, all the eight blocks were exploited until the discontinuation of financial supports and the transfer of the scheme management to the Water Users Association (WUA) in the early 1990s. The WUA is the local organization of farmers exploiting the KVIS, which comprises more than 1300 farmers as of 2018 (pers. comm. Lassané Kaboré). The scheme management transfer to the WUA led to a decline in maintenance works and the under and/or improper exploitation of the blocks, namely blocks 7 and 8 (Figure 1A) [32]. Examples of improper exploitation include the use of the soil as a construction material (i.e., bricks), which may have caused substantial soil fertility losses and affected the gravity-fed irrigation system. The KVIS has been fully operational again since 2009.

## 2.2. The Python Module for the Surface Energy Balance Algorithm for Land Model (PySEBAL)

The Python module for the Surface Energy Balance Algorithm for Land model (PySEBAL) (version 3.4.4.2) was developed by the IHE-Delft Institute for Water Education. It is freely available from <https://pypi.org/project/SEBAL/>. The PySEBAL model calculates the surface energy balance for the day that the satellite image was acquired independently from the land use [33,34], based on the inputs derived from the satellite images (i.e., NDVI, soil-adjusted vegetation index, soil emissivity, surface albedo, leaf area index, and surface temperature), along with weather and digital elevation model data. The outputs of PySEBAL include the actual evapotranspiration ( $ET_a$ ), crop coefficients ( $K_c$ ), and biomass at the daily time scale (i.e., day of RS image acquisition).

$ET_a$  values were derived as residuals of the surface energy balance. Crop coefficients were estimated as the ratios between  $ET_a$  and reference evapotranspiration ( $ET_0$ ), with the latter being calculated using the FAO-56 Penman–Monteith equation [35,36]. Daily biomass productions were estimated as a function of the fraction of absorbed photosynthetically active radiation, photosynthetically active radiation, and light use efficiency [37]. For more details on the SEBAL model and procedures to interpolate daily results between the periods and estimate dekadal (10-day period) and seasonal outputs, reference is made to [37–39].

One of the main advantages of the PySEBAL model is its automatic internal calibration, particularly regarding the selection of the driest and wettest pixels. The expected error from the automated calibration procedures when applied to climates in semiarid areas with dry summers (as was the case in this study) is approximately 10% less than that from a manual calibration carried out by experienced, cognizant users [40].

## 2.3. Comparisons of Estimated $ET_a$ Values Using PySEBAL to the FAO-WaPOR Products

Although the SEBAL model was found to satisfactorily estimate daily  $ET_a$  (deviations up to  $2.0 \text{ mm day}^{-1}$  when compared to ground data) over the savannah area of the Volta basin in West Africa, which encompasses our study area [41,42], in this study, before proceeding with the calculations of performance indicators and subsequent analyses, we assessed the quality of the estimated PySEBAL- $ET_a$  values by comparing them to those from FAO-WaPOR (version 1.0; [https://wapor.apps.fao.org/home/WAPOR\\_2/1](https://wapor.apps.fao.org/home/WAPOR_2/1)). FAO-WaPOR uses satellite data to produce agricultural land and water productivity data at three spatial levels: continental (250 m spatial resolution), country and river basin (100 m spatial resolution), and sub-national (30 m spatial resolution). Evapotranspiration values at different temporal scales are determined using the FAO-56 Penman–Monteith equation and satellite-derived data through the ETLook model. A description of the ETLook model is provided in [43]. The satellite data are from the Moderate Resolution Imaging Spectroradiometer (MODIS) and Advanced Microwave Scanning Radiometer (AMSRE) sensors. FAO-WaPOR data have been qualitatively assessed by checking the consistency of the different layers using various independent data sources [44]. Dekadal and seasonal  $ET_a$  data at a 250-m resolution for the study period were retrieved from the FAO-WaPOR's data portal (<https://wapor.apps.fao.org>). For the spatial comparison, PySEBAL- $ET_a$  data were resampled to a 250-m spatial resolution to match those of FAO-WaPOR using the nearest neighbor algorithm implemented in QGIS software (version 2.18.27). The root mean square error (RMSE) and the coefficient of determination ( $R^2$ ) were used as statistical indicators to assess the comparisons.

## 2.4. Irrigation Performance Indicators

Four performance indicators were evaluated in our study: depleted fraction, relative evapotranspiration ( $ET_{rel}$ ), uniformity of water consumption, and crop water productivity (CWP). These indicators were based on the lists proposed by the International Commission on Irrigation and Drainage [12,14,45]. Depleted fractions were estimated for the entire KVIS because of the lack of detailed irrigation supply data at the plot scale during the study period, and following the recommendations of [46,47] for such particular cases. The remaining three indicators (uniformity of water consumption,  $ET_{rel}$ , and CWP) were determined for each of the three crops.

### 2.4.1. Depleted Fraction

The depleted fraction is used to characterize the gross water balance of irrigable areas [46–48]. It was estimated as follows [48]:

$$\text{Depleted fraction} = \frac{ET_a}{\text{Rain} + V_c} \quad (1)$$

where Rain is the rainfall (mm) and  $V_c$  is the volume of irrigation supply (mm). Irrigation supply data of the main canal were used.

In this study, depleted fractions were calculated at a dekadal time step over January–April 2013 and 2014. Following [46], we assumed that depleted fractions ranging from 0.6 to 0.8 were indicative of good performance; the opposite for values less than 0.6.

### 2.4.2. Relative Evapotranspiration ( $ET_{rel}$ )

$ET_{rel}$  indicates the adequacy of water supply to avoid crop water stress [49]. It was estimated as follows:

$$ET_{rel} = \frac{ET_a}{ET_0} \quad (2)$$

where  $ET_a$  refers to the actual evapotranspiration (mm) estimated using PySEBAL and  $ET_0$  refers to the FAO-56 Penman–Monteith reference evapotranspiration (mm).

A common problem while determining  $ET_{rel}$  thresholds for performance indicators is the diversity of genotype responses according to the environment [50]. One genotype does not always have the same phenotypic characteristics in all environments. Likewise, different genotypes may respond differently to a specific environment [50,51]. Following previous studies [52–54], we considered an  $ET_{rel}$  equal to or greater than 0.75 as the threshold for a good performance. Values below 0.75 were indicative of poor performance.

### 2.4.3. Uniformity of Water Consumption

The uniformity of water consumption was described using the coefficient of variation (CV) of  $ET_a$  [55]. In our study, we adopted the ranges of CV values suggested by [20,49] to characterize the uniformity of water consumption across an irrigated area. An  $ET_a$  CV of less than 10 is indicative of a good uniformity of water consumption, whereas fair and poor uniformities of water consumption are indicated by  $ET_a$  CV values ranging from 10 to 25 and values greater than 25, respectively.

#### 2.4.4. Crop Water Productivity (CWP)

Different concepts of CWP exist. For instance, CWP can be defined as the ratio between a defined crop variable (e.g., yield) and the amount of water depleted (usually limited to crop evapotranspiration) [56], or as the gain in biomass or yield per unit of evapotranspiration or irrigation depth [57]. Following the latter definition, we referred to CWP in this study as the ratio between crop yield and  $ET_a$  (Equation (3)).

$$CWP = \frac{Yield}{ET_a} \quad (3)$$

The crop yield was estimated as a function of the biomass, harvest index, and crop grain (or tuber) moisture content at harvest (Equation (4)).

$$Yield = \frac{Biomass \times HI}{1 - Moist} \quad (4)$$

where Yield corresponds to grain or tuber yield ( $kg\ ha^{-1}$ ); HI is the harvest index (unitless); Biomass is the biomass estimated using PySEBAL ( $kg\ ha^{-1}$ ); and Moist is the moisture content of the crop grain (or tuber) at harvest (%). The harvest index values and grain/tuber moisture contents used in this study are presented in Section 2.5.3.

No official records of observed crop yields per plot were available during the study period because there were not regular updates of the crop yield databases every season. Only the average yields for the three crops recorded between 2008 and 2014 were provided. These values were 4.0, 2.5, and 15.7  $t\ ha^{-1}$  for paddy rice, maize, and sweet potato, respectively [8,58]. Thus, we did not carry out any detailed comparison analysis to evaluate the quality yield estimations using PySEBAL. To provide an idea of yield levels which could be expected given the common crop management practices across the KVIS (e.g., low fertilizer rates applied) and for comparison purposes, we considered the lowest values of potential yields provided by [59] (for rice) and [60] (for maize and sweet potato). That is, 5.0, 4.0, and 20.0  $t\ ha^{-1}$ , respectively, for paddy rice, maize, and sweet potato.

Various CWP values of rice, maize, and sweet potato were found in the literature, depending on the cultivars, cropping regions, and management practices. For example, the ranges of the CWP of rice and maize were 0.6 to 1.6  $kg\ m^{-3}$  and 1.2 to 2.3  $kg\ m^{-3}$  [61,62], respectively. Following the recommendations from [61,62], we assumed in this study CWP values of 0.6, 1.2, and 4  $kg\ m^{-3}$  as thresholds for rice, maize, and sweet potato, respectively, to characterize good performance. That is, CWP values less than the threshold were indicative of poor performance; the opposite for values equal to or greater than the threshold.

A schematic diagram describing the approach used in this study to assess the irrigation performance of the KVIS during the critical irrigation period (January–April) of the 2013 and 2014 cropping seasons is presented in Figure 2.

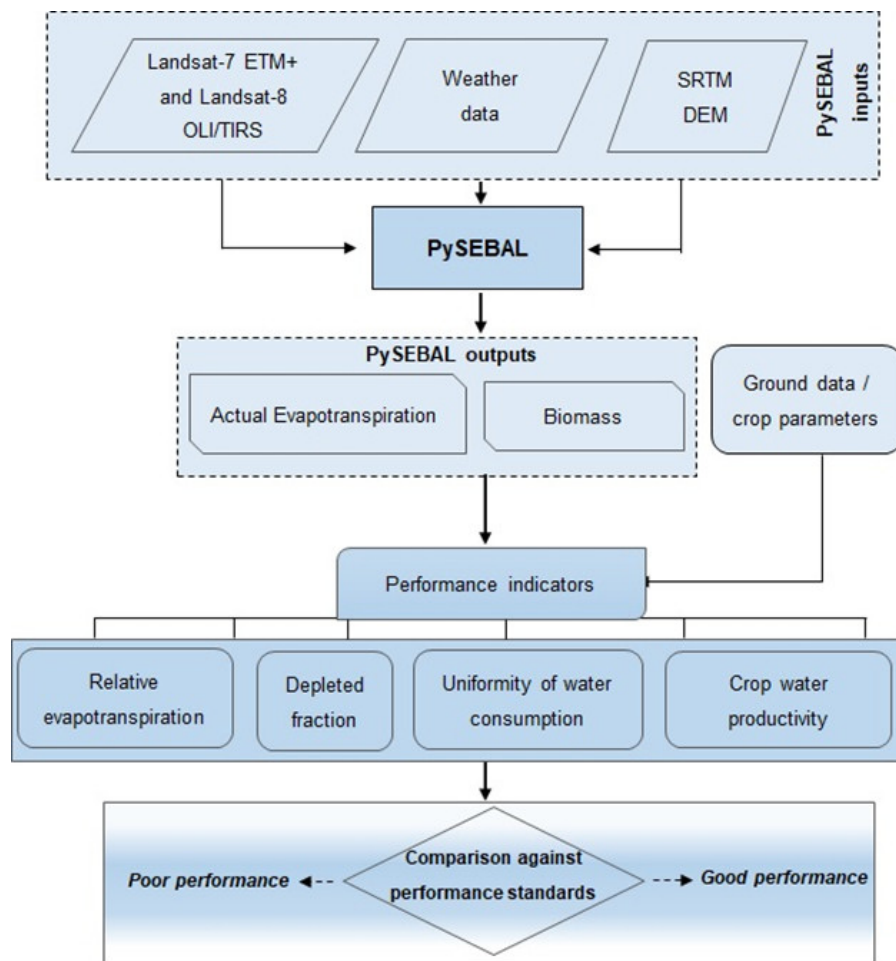


**Figure 2.** Schematic flowchart describing the approach used for assessing irrigation performance in the Kou Valley irrigation scheme.

## 2.5. Data

### 2.5.1. Landsat Images

Multi-temporal clear-sky images from the instruments Landsat-7 ETM+ and Landsat-8 Operational Land Imager (OLI) and Thermal Infrared Sensor (TIRS) were used in this study (Table 1). They were retrieved from the website <https://earthexplorer.usgs.gov/>. Data pre-processing, including data resampling (i.e., upscaling 100-m spatial resolution data to 30-m spatial resolution data), atmospheric corrections, the handling of digital elevation model (DEM) data, and cloud mask creation, was performed within PySEBAL [63].

**Table 1.** Landsat images from scene P197R052 used for assessing irrigation performance in the Kou Valley irrigation scheme during the study period 2013–2014.

Dry Season 2013			Dry Season 2014		
No.	Acquisition Date	Sensor <sup>1</sup>	No.	Acquisition Date	Sensor
1	02/01/2013	LE7	1	28/12/2013	LC8
2	18/01/2013	LE7	2	29/01/2014	LC8
3	03/02/2013	LE7	3	14/02/2014	LC8
4	07/03/2013	LE7	4	18/03/2014	LC8
5	08/04/2013	LE7	5	03/04/2014	LC8
6	09/04/2013	LC8	6	19/04/2014	LC8
7	03/06/2013	LC8	7	21/05/2014	LC8

<sup>1</sup> LE7: Landsat-7 ETM+. LC8: Landsat-8 OLI/TIRS. All data analyses and mapping were carried out using QGIS software (version 2.18.27) (<https://qgis.org/>) and ArcGIS software (version 10.4) [64].

Given the existence of wedge-shaped scan-to-scan gaps on both sides of each scene in Landsat-7 ETM+, with resulting data loss [65], these stripes were filled using the mask bands provided along with the downloaded data. In [66], it was pointed out that, for  $ET_a$  calculation from Landsat-7 ETM+ bands, filling the band gaps produces more consistent  $ET_a$  products within the stripe gaps than filling the final  $ET_a$  products. Hence, prior to  $ET_a$  calculations, the gaps in each Landsat-7 ETM+ band were filled using the Inverse Distance Weighting interpolation algorithm [67,68].

### 2.5.2. Weather and DEM Data

Weather data at 3-hourly and daily time steps for air temperature, wind speed, relative humidity, and solar radiation during 2013 and 2014 were used. Air temperature, wind speed, and relative humidity data were sourced from a synoptic weather station, located about 25 km southeast of the KVIS. Solar radiation data were retrieved from the website <http://www.soda-pro.com>. Daily weather data were used in REF-ET software (version 4.1) for calculating  $ET_0$  [36]. The 3-hourly weather data were used in PySEBAL for calculating  $ET_a$ .

DEM data at a 30-m spatial resolution were used in the correction process of surface temperature in PySEBAL, given the changes in temperatures according to elevation and slope. DEM data were sourced from the U.S. National Aeronautics and Space Administration (NASA) Shuttle Radar Topography Mission (SRTM).

### 2.5.3. Ground Data

Daily water flow rates (i.e., irrigation supply of the feeder canal of the KVIS), dekadal rainfall rates, HI, and grain/tuber moisture content for paddy rice, maize, and sweet potato were used. Water flow and rainfall rate data for the study period (Figure 3), measured at the feeder canal, were obtained from the management team of the KVIS [58]. Data of water lost by drainage and percolation were not available during the study period.

HI and grain/tuber moisture content data were retrieved from the literature [62,69–71]. HI and grain/tuber moisture contents (Table 2) were chosen within the range of reported values to reflect the common crop management practices across the KVIS.

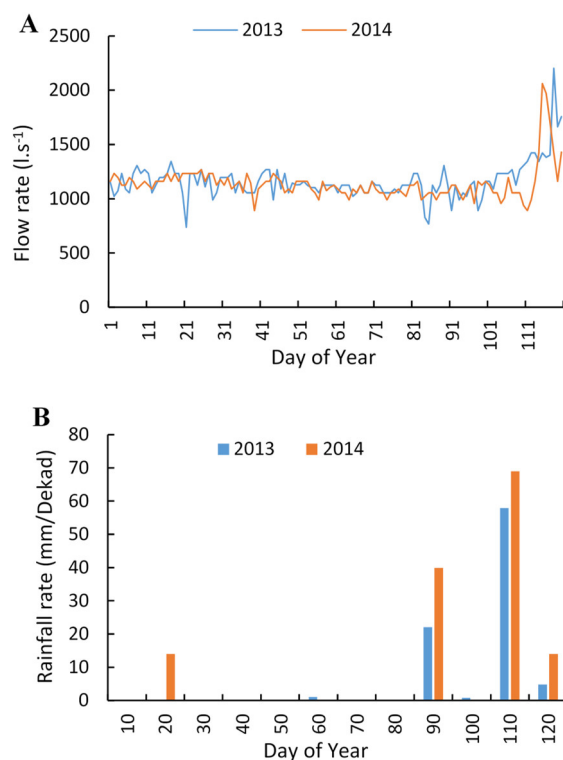


**Figure 3.** Water flow rates of the main canal (A) and rainfall rates (B) in the Kou Valley irrigation scheme during the study period.

**Table 2.** Values of harvest index (HI) and moisture content for paddy rice, maize, and sweet potato used in this study. HI and moisture contents were chosen to reflect the common crop management practices across the Kou Valley irrigation scheme.

Crops	HI (Unitless)		Moisture Content (%)		
	Reference		This Study	Reference	
	Values	Authors	Values	Values	Authors
Rice	0.40–0.50	[69]	0.45	15–20	[69]
Maize	0.30–0.40	[62]	0.35	18–24	[70]
Sweet Potato	0.75–0.85	[71]	0.8	75–80	[62]

The critical period of irrigation typically spans January to April, with rice nursery starting in December followed by transplantation in January. Maize sowing and sweet potato planting also occur in January. The growth cycles for maize, sweet potato, and rice cultivars vary between 80 and 100 days, 90 and 100 days, and 90 and 120 days, respectively. Harvests for all three crops generally take place in May. New Rice for Africa (NERICA) varieties (potential paddy yields of 5.0 to 7.0 t ha<sup>-1</sup>), maize composite varieties (i.e., Barka and Espoir; with potential yield levels ranging from 4.0 to 6.5 t ha<sup>-1</sup>), and local varieties of sweet potato (potential yield levels ranging from 20.0 to 30.0 t ha<sup>-1</sup>) were grown in the KVIS during the study period [59,60].

During the study period, rice was generally cultivated in the southern parts of the KVIS; maize plots were across the central to northeastern parts of the scheme; and sweet potato was mostly cultivated in the central parts of the scheme (Figure 4). The areas sown with rice, maize, and sweet potato were 452, 369, and 113 ha, respectively, during 2013. The respective values during 2014 were 317, 232, and 175 ha [58,72].

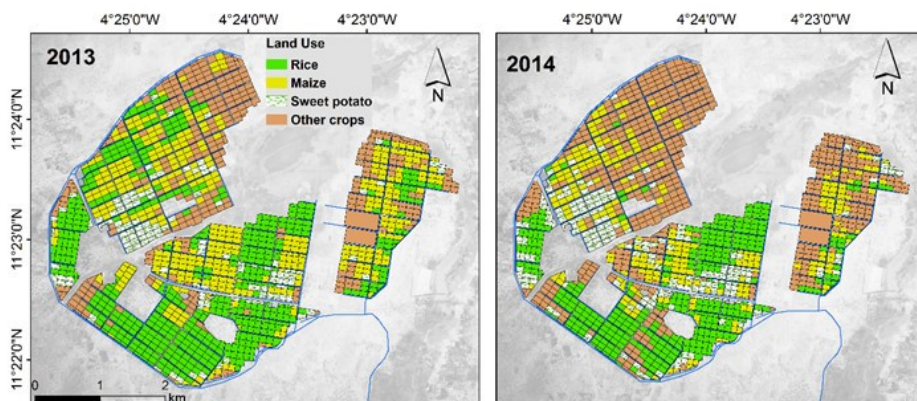


**Figure 4.** Land use across the Kou Valley irrigation scheme during the dry season production period in 2013 and 2014.

### 3. Results

#### 3.1. Comparisons between FAO-WaPOR and PySEBAL $ET_a$

The comparisons between FAO-WaPOR and PySEBAL  $ET_a$  at the dekadal and seasonal scales for the two dry season production periods are presented in Figure 5. For the 2013 period, PySEBAL seemed to slightly underestimate  $ET_a$  values at both temporal scales, with RMSE = 11 mm and 150 mm for the dekadal and seasonal estimations, respectively. In 2014, good agreements were found with RMSEs of 3.6 mm and 64 mm, and  $R^2$  of 0.74 and 0.70 for the dekadal and seasonal estimations, respectively (Figure 5). These results are in line with the reported conclusions of studies in Senegal, where  $ET_a$  values from flux towers were compared to FAO-WaPOR data [44]. FAO-WaPOR uses a global atmospheric model to supply meteorological data. The limitations of such a methodology include the uncertainties related to the spatial variability and spatial resolution of these data. For instance, temperature data have a spatial resolution of 0.25 degrees ( $\sim 28$  km at the equator). Data for atmospheric transmissivity have a 4-km spatial resolution, and Landsat images a 30-m spatial resolution for the bands used. Moreover, in FAO-WaPOR, gaps and anomalies are filled using a smoothing method, which can contribute to errors. Despite the underestimation observed in 2013, which can be related to these systematic errors within FAO-WaPOR [44,73], and, to some extent, to the quality of Landsat 7 ETM+ images, PySEBAL seemed to satisfactorily estimate  $ET_a$  values across the KVIS.

The relatively higher values of  $ET_a$  in 2014 (Figure 5) can be related to various factors, including crop management practices, water availability, and the weather. For instance, the difference in total cropped areas between 2013 and 2014 (934 ha and 724 ha, respectively) might have played a role in water availability to meet crop water needs during the study period, with more water virtually available in 2014. Although this could also explain the underestimation found with FAO-WaPOR in 2013, further research is required for a better understanding of such differences.

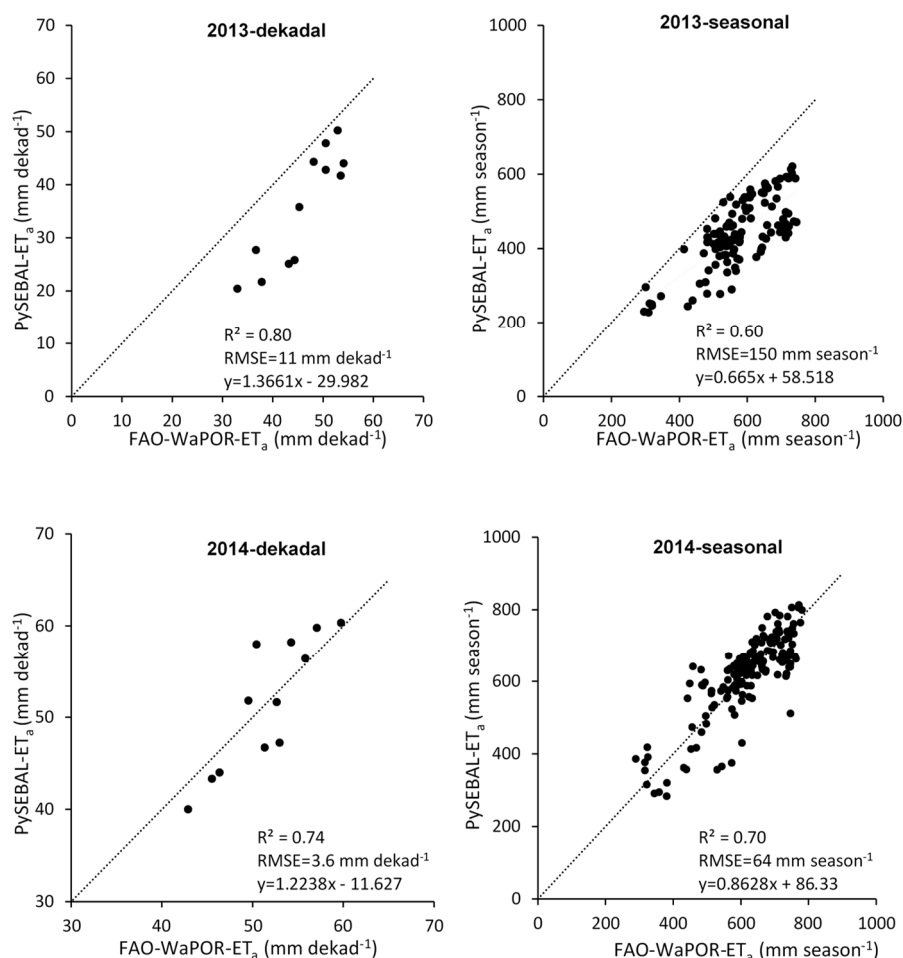


**Figure 5.** Comparisons between the Food and Agricultural Organization of the United Nations Water Productivity (FAO-WaPOR) and Python module for the Surface Energy Balance Algorithm for Land model (PySEBAL) derived actual evapotranspiration (ET<sub>a</sub>) at the dekadal and seasonal scales at the Kou Valley irrigation scheme during the dry season production period in 2013 and 2014. Comparisons at the dekadal scale were performed for the entire irrigation scheme, while those at the seasonal scale were performed on a pixel basis for the entire scheme. Dashed lines in the sub-figures represent the 1:1 line.

### 3.2. Seasonal Actual Evapotranspiration and Yield

Relatively higher ET<sub>a</sub> values were observed in 2014 compared to 2013. In 2014, the average value was 619 mm (range = 239–794 mm); in 2013, the average value was 554 mm (range = 178–750 mm) (Figure 6). When analyzing the results according to crop type, the average values were quite similar for maize and sweet potato plots, whereas those in rice plots were relatively higher. In 2013, the average ET<sub>a</sub> values were 551 and 546 mm in maize and sweet potato plots, respectively; the corresponding values in 2014 were 621 and 636 mm, respectively (Table 3; Figure 6). Values in rice plots were on average 635 and 709 mm in 2013 and 2014, respectively (Table 3; Figure 6). Between 2013 and 2014, ET<sub>a</sub> increased by up to 12%, 13%, and 16% for rice, maize, and sweet potato, respectively.

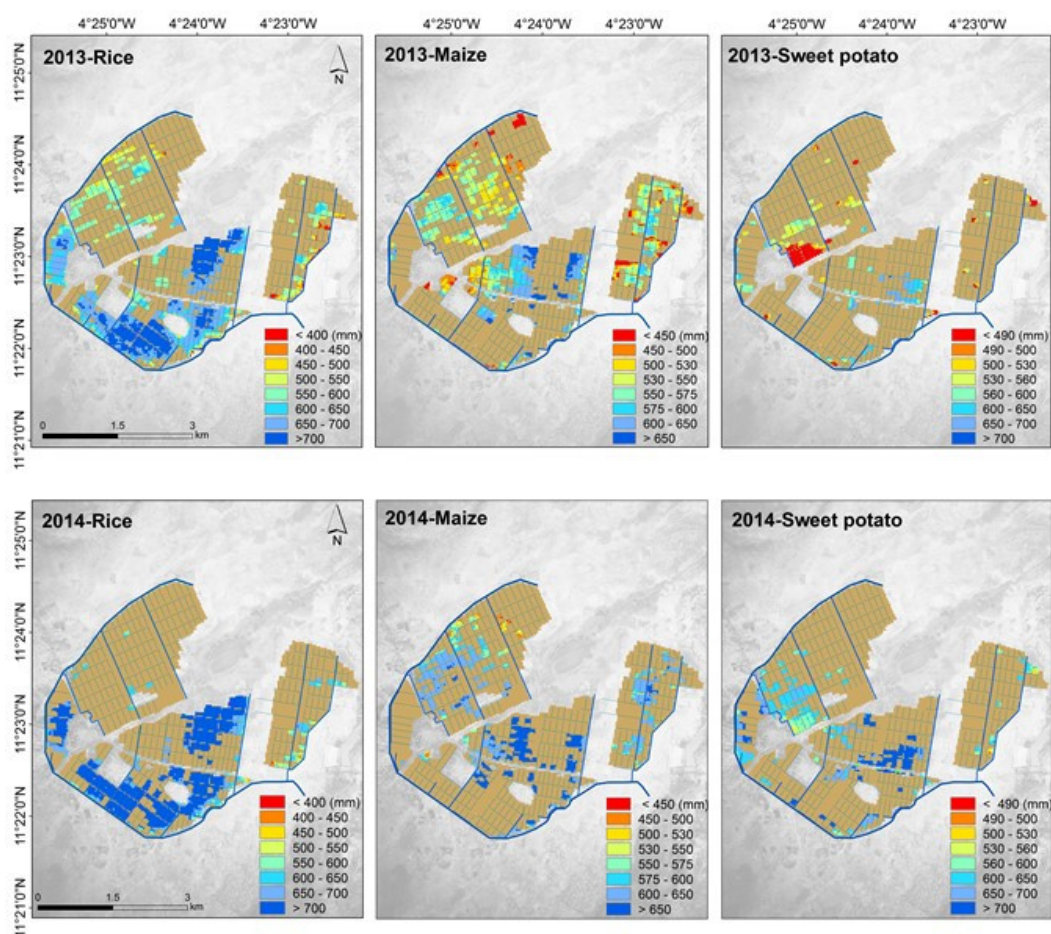


**Figure 6.** Seasonal  $ET_a$  for rice, maize, and sweet potato plots across the Kou Valley irrigation scheme during the dry season production period in 2013 and 2014.

**Table 3.** Ranges of estimated  $ET_a$  and yields for paddy rice, maize, and sweet potato during the dry season production periods in 2013 and 2014. The change rates of estimated  $ET_a$  and yields between 2013 and 2014 are provided.

		Rice	Maize	Sweet Potato
<b><math>ET_a</math> (mm)</b>				
<b>2013</b>	min	210	241	297
	mean	635	551	546
	max	750	713	712
<b>2014</b>	min	398	443	478
	mean	709	621	636
	max	793	750	778
Change rate (%)		+12	+13	+16
<b>Estimated yield (<math>t\ ha^{-1}</math>)</b>				
<b>2013</b>	min	0.40	0.40	6.10
	mean	3.39	2.20	12.0
	max	7.30	4.80	28.7
<b>2014</b>	min	1.30	0.70	6.50
	mean	4.20	2.30	18.4
	max	8.70	4.30	37.1
Change rate (%)		+23	+3	+53

The estimated yields were on average 2.2, 3.39, and 12.0,  $t\ ha^{-1}$  in 2013 for maize, paddy rice, and sweet potato, respectively (Table 3). In 2014, the respective estimated yields increased by up to 3%,

23%, and 53% (Table 3). The spatial distribution of the estimated yields for each of the crops during the two seasons is presented in Figure 7.

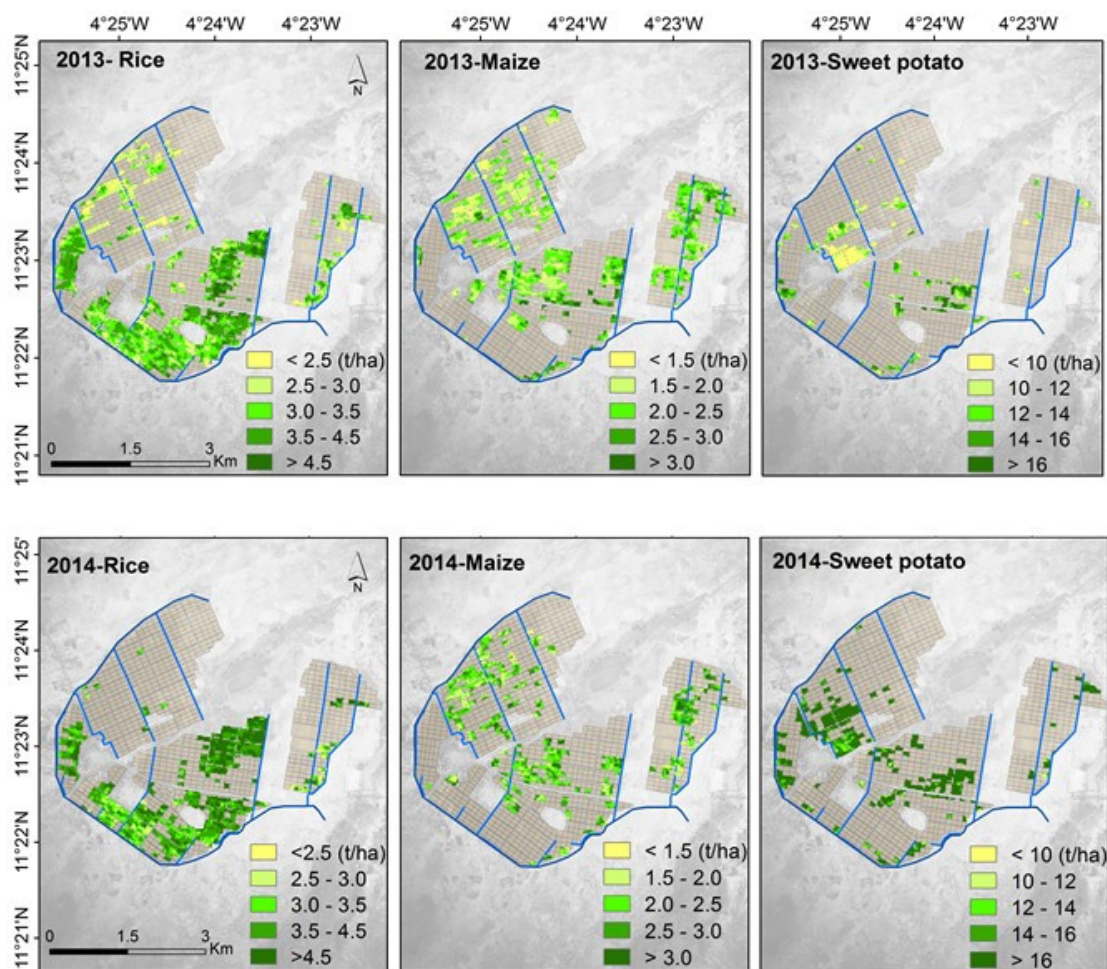


**Figure 7.** Estimated yields for rice, maize, and sweet potato plots across the Kou Valley irrigation scheme during the dry season production period in 2013 and 2014.

Comparing the estimated yields against the corresponding indicative values, the analysis shows mixed results depending on the year and crop (Table 4). For rice and sweet potato, there were areas across the KVIS where irrigation resulted in good performance, namely in 2014, with the estimated yields greater than the indicative standards. For instance, in 80% of the area planted with sweet potato in 2014, the estimated yield was greater or equal to the average yield observed during the 2008–2014 period (Table 4). Although the estimated maize yields were generally below the indicative standard in both years, there were plots in the southern parts of the irrigation scheme with estimated yields  $\geq 4.0 \text{ t ha}^{-1}$  (Figure 7). Note that in 2014, there were differences in rice transplanting dates for some plots (15 to 20% of plots concerned; pers. comm. Lassané Kaboré), resulting in differences in maturity and harvest dates. The yield estimates at the end of the monitoring period in 2014 thus did not include those plots.

**Table 4.** Ranges of estimated yield and proportions of crop areas with good performance in terms of yield for rice, maize, and sweet potato in the Kou Valley irrigation scheme during the dry season production periods in 2013 and 2014.

		Rice	Maize	Sweet Potato
Total pixels (count)	2013	5034	4069	1277
	2014	3540	2598	1940
Standards for good performance (SV) (t ha <sup>-1</sup> )		5.0	4.0	20.0
Proportion of pixels with values $\geq$ SV (%)	2013	2.0	0.3	0.7
	2014	18	0.2	31
Observed average yield (TY) (t ha <sup>-1</sup> )		4.0	2.5	15.7
Proportion of pixels with yield $\geq$ TY (%)	2013	17	18	12
	2014	54	37	80

### 3.3. Irrigation Performance Indicators

#### 3.3.1. Depleted Fractions

The KVIS was generally characterized by three temporal patterns of depleted fractions during each of the critical irrigation periods in 2013 and 2014 (Figure 8). Up to day of year (DOY) 65 in 2013 and DOY 50 in 2014, poor performance of the irrigation scheme was observed. This was followed by good performance from DOY 66 to 105 in 2013 and DOY 51 to 110 in 2014. Then, depleted fractions below 0.6 were again found during the late-season crop stages. At mid-season, with crops reaching in most cases their full leaf area development, there was an increase in  $ET_a$ . Depleted fractions greater than 0.6, as observed in both years, suggest a good use of irrigation water supply during the mid-season. During late-season crop stages, crop water needs decrease naturally because of leaf senescence. Irrigation supply was no longer required during this period, at least for the three major crops of maize, rice, and sweet potato.

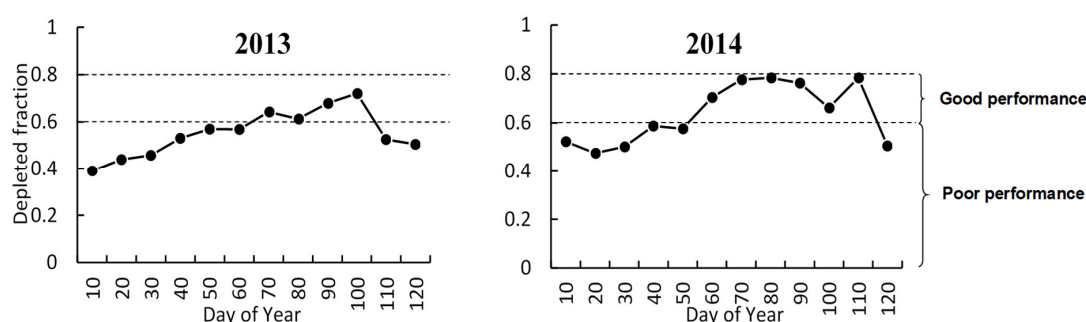


**Figure 8.** Variations of depleted fractions across the Kou Valley irrigation scheme during the dry season periods in 2013 and 2014. The thresholds for distinguishing between poor and good performance are indicated by the dashed lines.

#### 3.3.2. Relative Evapotranspiration

A northward gradient of spatially varying  $ET_{rel}$  was observed across the KVIS, resulting in four main crop areas according to the degree of water stress (Figure 9). Very highly water-stressed areas were dominant in the northern parts of the irrigation scheme (blocks 7 and 8). Highly water-stressed areas were found predominantly in the southern parts of the former areas (blocks 6 and 5). Across the central parts of the scheme, there were generally moderately water-stressed areas (block 4), and well-watered areas were observed in the southern parts of the irrigation scheme (blocks 2 and 3). Such variability can be related to soil types and the number of upstream water users. Indeed, around 25% of water supplied to the KVIS is lost due to the informal and uncontrolled water use upstream [3,27].

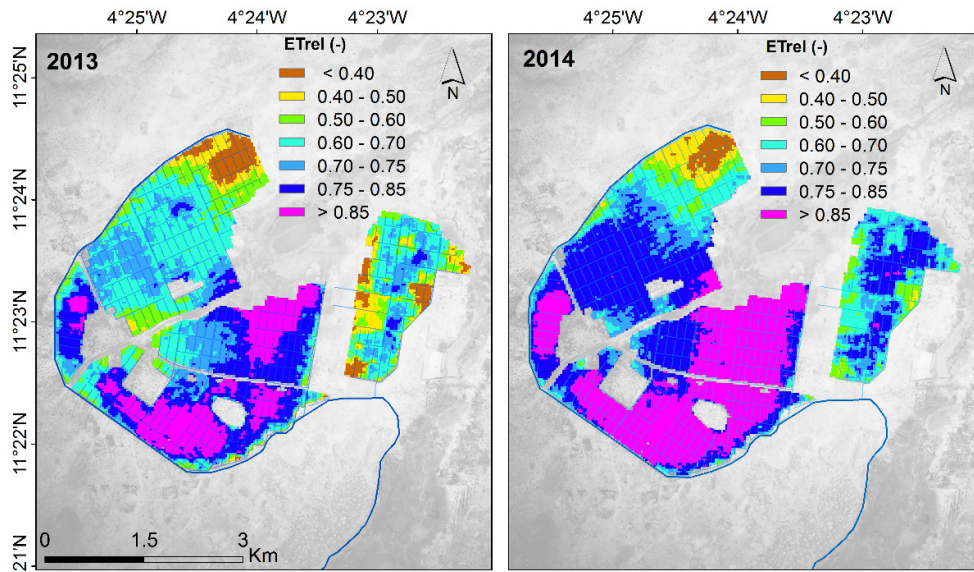


**Figure 9.** Spatial distribution of the seasonal relative evapotranspiration ( $ET_{rel}$ ) across the Kou Valley irrigation scheme during the dry season production period in 2013 and 2014.

When analyzing the  $ET_{rel}$  for each of the three crops, the results showed similar patterns for all crops: increasing  $ET_{rel}$  from the start to the end of the season for all crops in 2013 (Figure 10); slight decreases up to DOY 55, followed by an increasing trend for all crops in 2014 (Figure 10).  $ET_{rel}$  for maize and sweet potato was similar over most of the two seasons. In 2014, good indicators were generally observed for rice and sweet potato over the whole season (Figure 10). In 2013, good indicators ( $ET_{rel} > 0.75$ ) were found for rice from DOY 50 onwards. Those of maize and sweet potato were found a bit later in the season, from DOY 70 onwards. The decreases observed early in the 2014 season, at least for rice, can be attributed to the dissimilarity of growth stages across the irrigation scheme. Given the water scarcity observed in 2013, some farmers did not follow the recommended crop calendars for the 2014 cropping season, resulting in various sowing and transplanting dates, and subsequent uneven development. An example of rice plots with different growth stages across the KVIS during 2014 is presented in Figure S2.

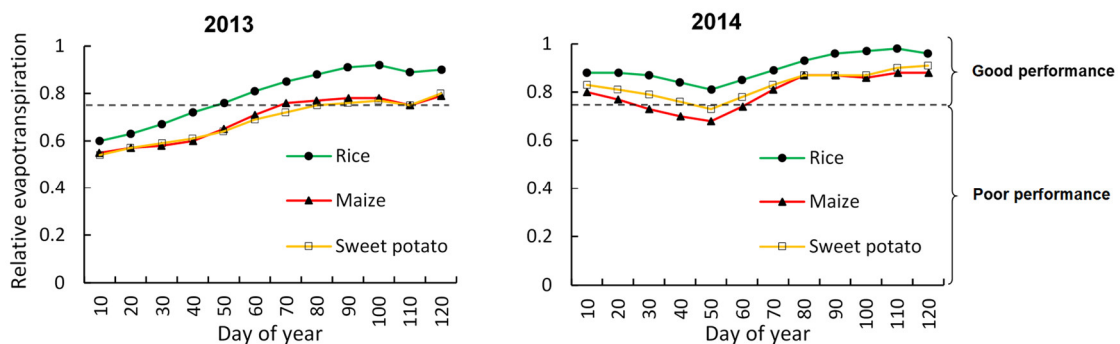


**Figure 10.** Variation of the relative evapotranspiration of paddy rice, maize, and sweet potato crops in KVIS during January–April 2013 and 2014. Dashed lines represent the thresholds for distinguishing between irrigated areas with poor or good performance.

### 3.3.3. Uniformity of Water Consumption

Different patterns of the uniformity of water consumption were observed depending on the year. In 2013, the uniformity of water consumption was fair for all crops (Figure 11). The variability of  $ET_a$  increased noticeably for sweet potato, from 10% to 20% CV, for DOY up to 100, before decreasing to 14% at around DOY 120. The variability of  $ET_a$  for maize and rice varied between 10% and 15% throughout the four-month monitoring period (Figure 11). In 2014, the variability of  $ET_a$  did not exceed 15% during the whole monitoring period. The patterns of uniformity of water consumption for all three crops were similar: fair uniformity up to DOY 60, followed by good uniformity from DOY 60 onwards (Figure 11). These results should be interpreted cautiously since water lost by drainage and percolation was not considered in the analysis due to the lack of such data during the study period.

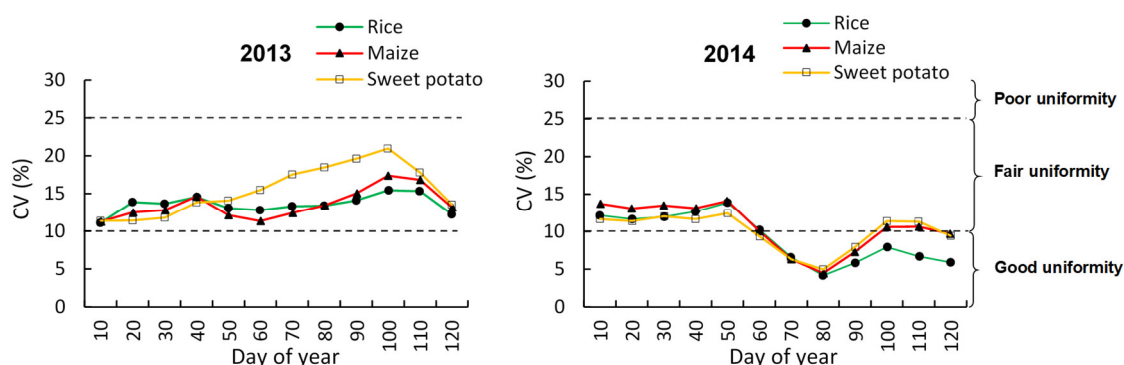


**Figure 11.** Variations of the uniformity of water consumption for paddy rice, maize, and sweet potato during January–April 2013 and 2014. The coefficient of variations (CV) of  $ET_a$  was used to characterize the uniformity of water consumption. Dashed lines represent the thresholds for distinguishing between irrigated areas with poor, fair, or good uniformity of water consumption.

### 3.3.4. Estimated Crop Water Productivities

Various CWP were observed across the KVIS according to the crop during the study period (Figure 12). In 2013, CWP were on average 0.53, 0.42, and 2.25  $\text{kg m}^{-3}$  for paddy rice, maize, and sweet potato, respectively (Figure 12; Table 5). In 2014, there was an increase in CWP for paddy rice and sweet potato, and a decrease for maize. The average values were 0.59, 0.38, and 2.89  $\text{kg m}^{-3}$  for rice, maize, and sweet potato, respectively (Figure 12; Table 5). Across the KVIS, there were plots with more than double the average CWP, irrespective of the crop. The maximum estimated CWP were 1.30  $\text{kg m}^{-3}$  for rice (estimated in 2014), 0.92  $\text{kg m}^{-3}$  for maize (estimated in 2013), and 5.86  $\text{kg m}^{-3}$  for sweet potato (estimated in 2014) (Figure 12; Table 5).

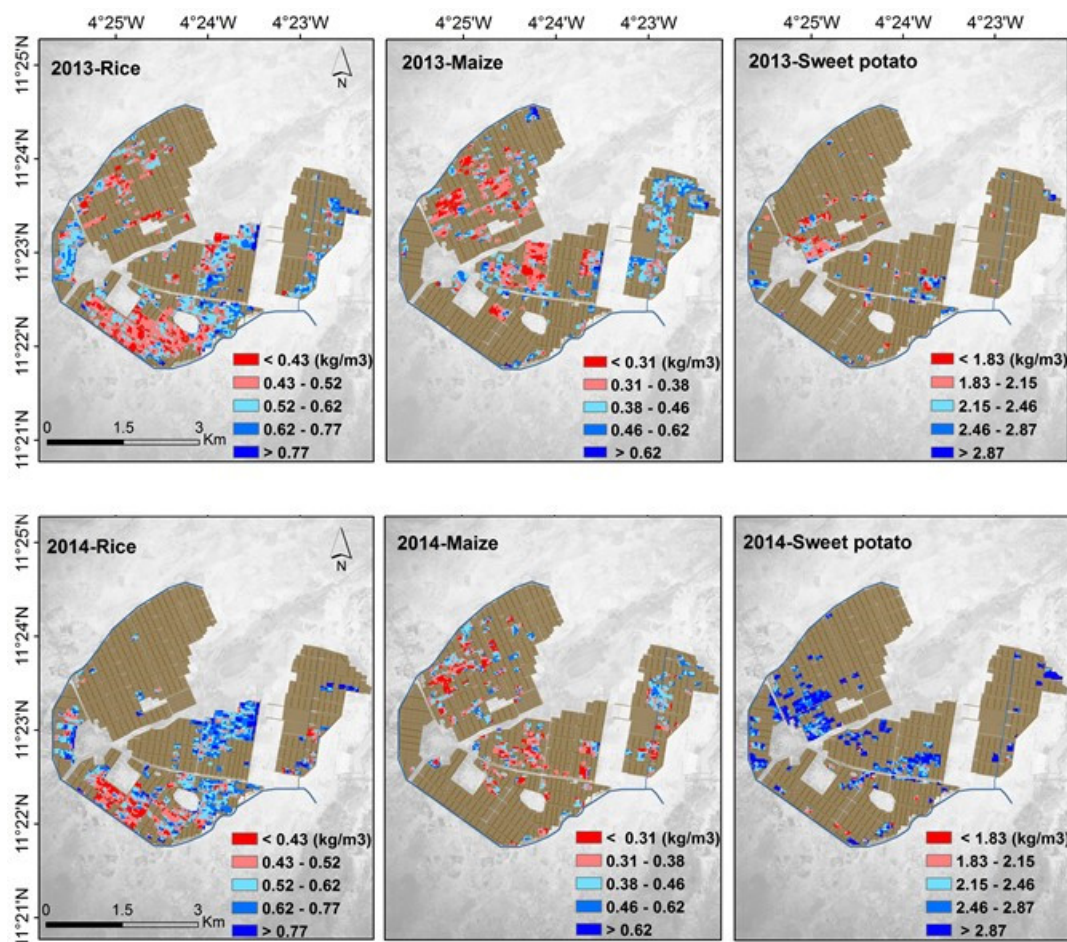


**Figure 12.** Spatial distributions of estimated crop water productivity for paddy rice, maize, and sweet potato across the Kou Valley irrigation scheme during the dry season production period in 2013 and 2014.

**Table 5.** Ranges of estimated crop water productivity (CWP), and proportions of crop areas with good irrigation performance in terms of CWP for rice, maize, and sweet potato in the Kou Valley irrigation scheme during the dry season production periods in 2013 and 2014.

			Rice	Maize	Sweet Potato
Range of estimated CWP	2013	min	0.15	0.10	1.02
		mean	0.53	0.42	2.25
		max	1.09	0.92	4.40
	2014	min	0.31	0.16	1.31
		mean	0.59	0.38	2.89
		max	1.30	0.76	5.86
Total pixels (count)	2013		5034	4069	1277
	2014		3540	2598	1940
Standards for good performance			0.60	1.20	4.00
Proportion of pixels with values $\geq$ SV (%)	2013		22	0	0.2
	2014		42	0	3

#### 4. Discussion

Using satellite RS-derived information, we assessed the spatial–temporal patterns of irrigation performance of the Kou Valley irrigation scheme during the dry season production periods in 2013

and 2014, based on four indicators. The comparison between the PySEBAL-estimated  $ET_a$  for maize and reported values shows good agreement. In [74], a range of 200–1000 mm for  $ET_a$  in irrigated maize was reported in their review. In this study, the corresponding range was 241–750 mm during the two seasons (Table 3). That of rice (210–793 mm; Table 3) was relatively below the reported range of 400–800 mm [74]. Such low  $ET_a$  values for rice can be related to the differences in cultivars and crop management practices.

Conversely, whilst the estimated CWP<sub>s</sub> for rice were similar to those reported in previous studies [16,74,75], those for maize were lower compared to the average values reported by [74] (the range being from 1.1 to 2.7 kg m<sup>-3</sup>). Such differences can be related to differences in soil fertility, crop management practices, and water availability during the study period. Considering the optimum values of key nutrient rates and irrigation water to maximize CWP [74], the typically low rates of nutrients (i.e., urea and blended NPK) applied across the KVIS [16,75] could have explained the CWP found in this study. Furthermore, crop yields were estimated using fixed HI values in PySEBAL, which implies a linear relationship between biomass production and yields. However, under field conditions, biomass production and harvest index varied depending on the timing and the magnitude of biotic and abiotic stresses [40,76]. Using fixed HI values could have led to biases in the estimated crop yields. Hence, the estimated values and related indicators must be considered as indicative and interpreted cautiously. Nevertheless, the consistency of our results with those derived from field data, at least for rice [16,75], showed that the RS-based approach can be an alternative for the time- and cost-efficient assessment of irrigation performance in the study region.

Low values for depleted fractions were observed during the study period, suggesting noticeable water losses through drainage and percolation. The continuous flow of water for irrigation from the Kou River, coupled with the irrigation method practiced in the KVIS, was conducive to such losses, particularly during the growth stages with low water requirements. There is a need for alternative water-saving methods, such as equipping farmers with more water storage systems to better handle water excess. Soil types, water availability, and crop and water management practices affected the actual and relative evapotranspiration across the KVIS. A follow-up analysis related to the relationships between the spatial variability of the relative evapotranspiration, soil types, DEM, and plot distance from the scheme inlet analysis is underway. The outcomes of this analysis will be the subject of an upcoming paper.

Maize was initially promoted across the KVIS to help farmers face water scarcity [29]. However, this crop did not reach its full potential during the study period: values greater than or equal to the target average yield were found in only 18% (2013) and 37% (2014) of land areas planted with maize (Table 4). Similar results were observed for rice in 2013. In 2014, sweet potato outperformed the two other crops in terms of areas with good yields. The poor performance achieved by maize and rice seems to have been captured by farmers, with less areas planted with rice or maize between 2013 and 2014 (~30% and 36% decrease for rice and maize, respectively) and more areas planted with sweet potato (52% increase between the two years) (see total pixel count in Table 4). There are opportunities to improve maize and rice productivity through a better management of fertilization and a compliance to recommended crop calendars.

This study focused on diagnostic performance indicators with the purpose of detecting areas with good and poor performance across the KVIS. Because of a lack of observations, comparisons were performed using indicative standard values, calling for caution in the interpretation of such results. In [77,78], region-specific optimal CWP values when setting benchmarks for comparison purposes are recommended. Various reasons, including climate conditions and soil properties, can affect CWP from one region to another [77]. Moreover, it remains unclear whether a higher CWP value in one location indicates a more desirable situation than a lower CWP value in another location [77]. Future research could aim at determining benchmark CWP values under local conditions across the KVIS for improving such a performance assessment.

The ranges of irrigation performance indicators found for the KVIS highlight the various issues encountered across this scheme, as well as the challenges for its good management. Such insightful information about the spatio-temporal patterns of irrigation performance can help in engaging with the WUA for an improved management of the irrigation scheme. Furthermore, the methodology applied in this study could be replicated readily using different sources of RS satellite images, such as Copernicus-Sentinel-2 or Copernicus-Sentinel-1, in combination with radar imaging to enable better  $ET_a$  estimations under cloudy conditions. Despite the potential of such a methodology to help managers and other decision makers improve water management in data-scarce areas, the success of RS applications for land and irrigation water management remains limited in Burkina Faso for various reasons. Irrigation scheme managers, consultants, and policy makers are usually not aware of such opportunities [14] or the products developed are often not user driven [79]. To overcome this challenge, more case studies involving all the stakeholders (from farmers to scheme managers to policy makers) need to be undertaken to increase their awareness and build and/or strengthen their capacity. Such activities can be done through the existing private–public partnerships [3]. Another solution to overcome barriers for adopting such RS-based methodologies could be the implementation of RS and GIS units within the scheme management services.

## 5. Conclusions

Given the increasing pressure on water for agricultural irrigation, coupled with unpredictable climate conditions, and with the lack of resources to carry out regular performance assessment for irrigation schemes, the use of cost-effective methodologies is critically important to improve irrigation water management and sustain crop production. We investigated the irrigation performance of the Kou Valley irrigation scheme during the dry season cultivation periods in 2013 and 2014 based on four indicators derived from Landsat satellite images. Employing the PySEBAL model, irrigation performance indicators, such as the depleted fraction, relative evapotranspiration, uniformity of water consumption, and crop water productivity for three crops (maize, rice, and sweet potato), were computed to provide more insights into the spatio-temporal patterns of the irrigation performance. The study showed spatially different crop areas depending on the level of water stress (from very high water stress to moderately stressed to well-watered crop areas) across the KVIS, with below-par performance according to each crop. It also indicated that irrigation water management needs to be improved, namely during the early and late crop phenological stages. Such findings could guide the management team and farmers' organizations for appropriate measures to improve the overall performance of the irrigation scheme with the aim to increase crop yields and farmers' incomes.

**Supplementary Materials:** The following are available online at <http://www.mdpi.com/2220-9964/9/8/484/s1>. Figure S1: The Kou watershed: its water resources and users. Source: Adapted from [27], Figure S2: Different growth stages of rice observed during the 2014 cropping season in the Kou Valley irrigation scheme.

**Author Contributions:** Conceptualization, Alidou Sawadogo and Kemal Sulhi Gündoğdu; PySEBAL model application, Alidou Sawadogo and Tim Hessels; Formal analysis, Alidou Sawadogo; Writing—original draft preparation, Alidou Sawadogo; Writing—review and editing, Louis Kouadio, Farid Traoré, Sander J. Zwart, and Kemal Sulhi Gündoğdu. All authors have read and agreed to the published version of the manuscript.

**Funding:** The first author (A.S.) was supported by the Presidency for Turks Abroad and Related Communities (YTB) fund.

**Acknowledgments:** We are grateful to the managers of the Kou Valley irrigation scheme, particularly Lassané Kaboré for sharing the crop yield and management data. We also thank Abebe Chukalla for the constructive comments on an earlier version of this manuscript.

**Conflicts of Interest:** The authors declare no conflicts of interest.

## References

1. Blatchford, M.L.; Karimi, P.; Bastiaanssen, W.G.M.; Nouri, H. From Global Goals to Local Gains—A Framework for Crop Water Productivity. *ISPRS Int. J. Geo-Inf.* **2018**, *7*, 414. [[CrossRef](#)]

2. Stoyanova, A.; Stoyanova, D. Study on the Productivity of Irrigation Water at Maize (*Zea Mays*). *Acta Sci. Agric.* **2019**, *3*, 51–55.
3. Wellens, J.; Nitchou, M.; Traore, F.; Tychon, B. A public-private partnership experience in the management of an irrigation scheme using decision-support tools in Burkina Faso. *Agric. Water Manag.* **2013**, *116*, 1–11. [[CrossRef](#)]
4. De Bruin, H.; Stricker, J. Evaporation of grass under non-restricted soil moisture conditions. *Hydrol. Sci. J.* **2000**, *45*, 391–406. [[CrossRef](#)]
5. Turner, K.; Georgiou, S.; Clark, R.; Brouwer, R.; Burke, J. *Economic Valuation of Water Resources in Agriculture. From the Sectoral to a Functional Perspective of Natural Resource Management*; Volume Water Reports 27; United Nations Food and Agriculture Organization (FAO): Rome, Italy, 2004.
6. Waller, P.; Yitayew, M. Introduction. In *Irrigation and Drainage Engineering*; Waller, P., Yitayew, M., Eds.; Springer International Publishing: Cham, Switzerland, 2016; pp. 1–18. [[CrossRef](#)]
7. Poussin, J.C.; Renaudin, L.; Adogoba, D.; Sanon, A.; Tazen, F.; Dogbe, W.; Fusillier, J.L.; Barbier, B.; Cecchi, P. Performance of small reservoir irrigated schemes in the Upper Volta basin: Case studies in Burkina Faso and Ghana. *Water Resour. Rural Dev.* **2015**, *6*, 50–65. [[CrossRef](#)]
8. FAO. *Country Fact Sheet on Food and Agriculture Policy Trends—Burkina Faso, April 2014*; United Nations Food and Agriculture Organization (FAO): Rome, Italy, 2014.
9. Traoré, F.; Bonkougou, J.; Compaoré, J.; Kouadio, L.; Wellens, J.; Hallot, E.; Tychon, B. Using multi-temporal landsat images and support vector machine to assess the changes in agricultural irrigated areas in the Mogtedo region, Burkina Faso. *Remote Sens.* **2019**, *11*, 1442. [[CrossRef](#)]
10. Gorantiwar, S.D.; Smout, I.K. Performance assessment of irrigation water management of heterogeneous irrigation schemes: 1. A framework for evaluation. *Irrig. Drain. Syst.* **2005**, *19*, 1–36. [[CrossRef](#)]
11. Murray-Rust, D.H.; Snellen, W.B. *Irrigation system Performance Assessment and Diagnosis*; International Irrigation Management Institute: Colombo, Sri Lanka, 1993.
12. Bos, M.G. Performance indicators for irrigation and drainage. *Irrig. Drain. Syst.* **1997**, *11*, 119–137. [[CrossRef](#)]
13. Bos, M.G.; Burton, M.A.; Molden, D.J. *Irrigation and Drainage Performance Assessment—Practical Guidelines*; CABI Publishing: Wallingford, UK; Cambridge, MA, USA, 2005; p. 166. [[CrossRef](#)]
14. Bastiaanssen, W.G.M.; Bos, M.G. Irrigation Performance Indicators Based on Remotely Sensed Data: A Review of Literature. *Irrig. Drain. Syst.* **1999**, *13*, 291–311. [[CrossRef](#)]
15. Dembélé, Y.; Ouattara, S.; Keïta, A. Application des indicateurs “approvisionnement relatif en eau” et “productivité de l’eau” à l’analyse des performances des petits périmètres irrigués au Burkina Faso. *Irrig. Drain.* **2001**, *50*, 309–321. [[CrossRef](#)]
16. Dembélé, Y.; Yacouba, H.; Keïta, A.; Sally, H. Assessment of irrigation system performance in south-western Burkina Faso. *Irrig. Drain.* **2012**, *61*, 306–315. [[CrossRef](#)]
17. Kambou, D.; Degre, A.; Xanthoulis, D.; Ouattara, K.; Destain, J.P.; Defoy, S.; De L’escaille, D. Evaluation and Proposals for Improving Irrigation Performance Around Small Reservoirs in Burkina Faso. *J. Irrig. Drain. Eng.* **2019**, *145*, 05019004. [[CrossRef](#)]
18. Somé, L.; Dembélé, Y. Péjoration climatique au Burkina Faso: Impacts sur les productions agricoles. In *Proceedings of the Recherches Scientifique Face Aux Problèmes de L’environnement. Actes de la 2ème Édition du Forum National de la Recherche Scientifique et Technologique, Ouagadougou, Burkina Faso, 9–13 April 1996*; pp. 81–89.
19. Blatchford, M.L.; Mannaerts, C.M.; Zeng, Y.; Nouri, H.; Karimi, P. Status of accuracy in remotely sensed and in-situ agricultural water productivity estimates: A review. *Remote Sens. Environ.* **2019**, *234*, 111413. [[CrossRef](#)]
20. Bastiaanssen, W.G.M.; Brito, R.A.L.; Bos, M.G.; Souza, R.A.; Cavalcanti, E.B.; Bakker, M.M. Low cost satellite data for monthly irrigation performance monitoring: Benchmarks from Nilo Coelho, Brazil. *Irrig. Drain. Syst.* **2001**, *15*, 53–79. [[CrossRef](#)]
21. Zwart, S.J.; Leclert, L.M.C. A remote sensing-based irrigation performance assessment: A case study of the Office du Niger in Mali. *Irrig. Sci.* **2010**, *28*, 371–385. [[CrossRef](#)]
22. Taghvaeian, S.; Neale, C.M.; Osterberg, J.C.; Sritharan, S.I.; Watts, D.R. Remote sensing and gis techniques for assessing irrigation performance: Case study in Southern California. *J. Irrig. Drain. Eng.* **2018**, *144*, 05018002. [[CrossRef](#)]

23. Bandara, K.M.P.S. Monitoring irrigation performance in Sri Lanka with high-frequency satellite measurements during the dry season. *Agric. Water Manag.* **2003**, *58*, 159–170. [[CrossRef](#)]
24. Akbari, M.; Toomanian, N.; Droogers, P.; Bastiaanssen, W.; Gieske, A. Monitoring irrigation performance in Esfahan, Iran, using NOAA satellite imagery. *Agric. Water Manag.* **2007**, *88*, 99–109. [[CrossRef](#)]
25. Ahmad, M.D.; Turrall, H.; Nazeer, A. Diagnosing irrigation performance and water productivity through satellite remote sensing and secondary data in a large irrigation system of Pakistan. *Agric. Water Manag.* **2009**, *96*, 551–564. [[CrossRef](#)]
26. Guinko, S. *Végétation de Haute Volta*. Ph.D. Thesis, Université de Bordeaux, Bordeaux, France, 1984.
27. Traoré, F. *Optimisation de l'utilisation des Ressources en eau du Bassin du Kou Pour des Usages Agricoles*. Ph.D. Thesis, Université de Liège, Liège, Belgium, 2012.
28. Traoré, F.; Cornet, Y.; Denis, A.; Wellens, J.; Tychon, B. Monitoring the evolution of irrigated areas with Landsat images using backward and forward change detection analysis in the Kou watershed, Burkina Faso. *Geocarto Int.* **2013**, *28*, 733–752. [[CrossRef](#)]
29. Wellens, J.; Diallo, M.; Compaore, N.F.; Derouane, J.; Tychon, B. *Renforcement Structurel de la Capacité de Gestion des Ressources en eau Pour L'agriculture Dans le Bassin du Kou; Rapport Technique 1 (2005–2006)*; APEFE-WBI: Bobo-Dioulasso, Burkina Faso, 2007.
30. Ouédraogo, S. *Analyse Économique de L'allocation des Facteurs de Production Dans Les Exploitations Rizicoles de la VALLÉE du Kou*; CNRST/INERA: Ouagadougou, Burkina Faso, 1993.
31. Dicko, D. *Evaluation des Performances Sur le Périmètre de la Vallée du Kou*; Projet APPIA-EIERGEeau: Ouagadougou, Burkina Faso, 2004.
32. Wellens, J.; Diallo, M.; Nitchou, M.; Traoré, F.; Midekor, A.; Sawadogo, B.; Tychon, B. Appropriation of decision support tools derived results in the public-private management of an irrigation scheme in Burkina Faso. In *Proceedings of the Conférence Watarid 3—Usages et Politiques de L'eau en Zones Arides et Semi-Arides*, Paris, France, 30 May–5 June 2011; p. 563.
33. Bastiaanssen, W.G.M.; Menenti, M.; Feddes, R.A.; Holtslag, A.A.M. A remote sensing surface energy balance algorithm for land (SEBAL). 1. Formulation. *J. Hydrol.* **1998**, *212–213*, 198–212. [[CrossRef](#)]
34. Bastiaanssen, W.G.M.; Ahmad, M.-D.; Chemin, Y. Satellite surveillance of evaporative depletion across the Indus Basin. *Water Resour. Res.* **2002**, *38*, 1273. [[CrossRef](#)]
35. Allen, R.G.; Pereira, L.S.; Raes, D.; Smith, M. *Crop Evapotranspiration: Guidelines for Computing Crop Water Requirements*; Volume Irrigation and Drainage Paper No. 56; Food and Agriculture Organization of the United Nations (FAO): Rome, Italy, 1998; p. 300.
36. Allen, R.G. *REF-ET: Reference Evapotranspiration Calculation Software for FAO and ASCE Standardized Equations. Reference Manual*; University of Idaho: Kimberly, ID, USA, 2016.
37. Bastiaanssen, W.G.M.; Ali, S. A new crop yield forecasting model based on satellite measurements applied across the Indus Basin, Pakistan. *Agric. Ecosyst. Environ.* **2003**, *94*, 321–340. [[CrossRef](#)]
38. Zwart, S.J.; Bastiaanssen, W.G.M. SEBAL for detecting spatial variation of water productivity and scope for improvement in eight irrigated wheat systems. *Agric. Water Manag.* **2007**, *89*, 287–296. [[CrossRef](#)]
39. Trezza, R.; Allen, R.G.; Kilic, A.; Ratcliffe, I.; Tasumi, M. Influence of Landsat revisit frequency on time-integration of evapotranspiration for agricultural water management. In *Advanced Evapotranspiration Methods and Applications*; Bucur, D., Ed.; IntechOpen: London, UK, 2018. [[CrossRef](#)]
40. Musick, J.T.; Jones, O.R.; Stewart, B.A.; Dusek, D.A. Water-yield relationships for irrigated and dryland wheat in the US Southern Plains. *Agron. J.* **1994**, *86*, 980–986. [[CrossRef](#)]
41. Compaoré, H.; Hendrickx, J.M.H.; Hong, S.; Friesen, J.; van de Giesen, N.C.; Rodgers, C.; Szarzynski, J.; Vlek, P.L.G. Evaporation mapping at two scales using optical imagery in the White Volta Basin, Upper East Ghana. *Phys. Chem. Earth Parts A/B/C* **2008**, *33*, 127–140. [[CrossRef](#)]
42. Opoku-Duah, S.; Donoghue, N.M.D.; Burt, P.T. Intercomparison of evapotranspiration over the savannah Volta Basin in West Africa using remote sensing data. *Sensors* **2008**, *8*, 2736–2761. [[CrossRef](#)]
43. Bastiaanssen, W.G.M.; Cheema, M.J.M.; Immerzeel, W.W.; Miltenburg, I.J.; Pelgrum, H. Surface energy balance and actual evapotranspiration of the transboundary Indus Basin estimated from satellite measurements and the ETLook model. *Water Resour. Res.* **2012**, *48*, W11512. [[CrossRef](#)]
44. FAO; IHE Delft. *WaPOR Quality Assessment: Technical Report on the Data Quality of the WaPOR FAO Database Version 1.0*; FAO: Rome, Italy, 2019; p. 134.

45. UNDESAPD. *World Urbanization Prospects: The 2014 Revision, Highlights (ST/ESA/SER.A/352)*; United Nations: New York, NY, USA, 2014.
46. Bos, M.G. Using the depleted fraction to manage the groundwater table in irrigated areas. *Irrig. Drain. Syst.* **2004**, *18*, 201–209. [[CrossRef](#)]
47. Bos, M.G.; Kselik, R.A.; Allen, R.G.; Molden, D. *Water Requirements for Irrigation and the Environment*; Springer: Dordrecht, The Netherlands, 2009; p. 174. [[CrossRef](#)]
48. Molden, D. *Accounting for Water Use and Productivity*; Volume IWMI/SWIM Paper No. 1; International Water Management Institute: Colombo, Sri Lanka, 1997.
49. Molden, D.J.; Gates, T.K. Performance measures for evaluation of irrigation-water-delivery systems. *J. Irrig. Drain. Eng.* **1990**, *116*, 804–823. [[CrossRef](#)]
50. Kang, M.S. Using genotype-by-environment interaction for crop cultivar development. In *Advances in Agronomy*; Sparks, D.L., Ed.; Academic Press: Cambridge, MA, USA, 1997; Volume 62, pp. 199–252.
51. Gallais, A. *Théorie de la Sélection en Amélioration des Plantes*; Masson: Paris, France; Milan, Italy; Barcelona, Spain, 1990.
52. Roerink, G.J.; Bastiaanssen, W.G.M.; Chambouleyron, J.; Menenti, M. Relating crop water consumption to irrigation water supply by remote sensing. *Water Resour. Manag.* **1997**, *11*, 445–465. [[CrossRef](#)]
53. Asaana, J.; Sadick, A. Assessment of irrigation performance using remote sensing technique at Tono irrigation area in the Upper East region of Ghana. *Int. Res. J. Agric. Food Sci.* **2016**, *1*, 79–91.
54. Akhtar, F.; Awan, U.K.; Tischbein, B.; Liaqat, U.W. Assessment of irrigation performance in large river basins under data scarce environment—A case of Kabul river basin, Afghanistan. *Remote Sens.* **2018**, *10*, 972. [[CrossRef](#)]
55. Bastiaanssen, W.G.M.; van der Wal, T.; Visser, T.N.M. Diagnosis of regional evaporation by remote sensing to support irrigation performance assessment. *Irrig. Drain. Syst.* **1996**, *10*, 1–23. [[CrossRef](#)]
56. Kijne, J.W.; Barker, R.; Molden, D. Improving water productivity in agriculture: Editors' overview. In *Water Productivity in Agriculture: Limits and Opportunities for Improvement*; Kijne, J.W., Barker, R., Molden, D., Eds.; CABI and International Water Management Institute (IWMI): Wallingford, UK; Colombo, Sri Lanka, 2003.
57. Perry, C.; Steduto, P.; Allen, R.G.; Burt, C.M. Increasing productivity in irrigated agriculture: Agronomic constraints and hydrological realities. *Agric. Water Manag.* **2009**, *96*, 1517–1524. [[CrossRef](#)]
58. DRASA-Ouest. *Production Saisonnière Sur la Plaine de la Vallée du Kou de 2008 à 2014*; Direction Régionale de L'agriculture et de la Sécurité Alimentaire (DRASA): Ouagadougou, Burkina Faso, 2014.
59. Dembélé, Y.; Dakouo, D.; Ouedraogo, J.; Siambo, E.; Traoré, Y.; Nishiyama, N. Creation et diffusion des variétés type NERICA au Burkina Faso. In Proceedings of the Atelier Conjoint Pour Une Riziculture Durable en Afrique, Accra, Ghana, 6–9 December 2006.
60. MASA. *Catalogue National des Espèces et Variétés Agricoles du Burkina Faso. Première Édition Comité National des Semences*; Ministère de l'Agriculture et de la Sécurité Alimentaire (MASA): Ouagadougou, Burkina Faso, 2014.
61. FAO. *Unlocking the Water Potential of Agriculture*; United Nations Food and Agriculture Organization (FAO): Rome, Italy, 2003.
62. Steduto, P.; Hsiao, C.T.; Fereres, E.; Raes, D. *Crop Yield Response to Water*; Volume FAO Irrigation and Drainage Paper No. 66; United Nations Food and Agriculture Organization (FAO): Rome, Italy, 2012; p. 505.
63. Hessels, T.; van Opstal, J.; Trambauer, P.; Bastiaanssen, W.G.M.; Fauzi, M.; Mohamed, Y.; Er-Raji, A. pySEBAL Version 3.3.7. 2017. Available online: <https://pypi.org/project/SEBAL/> (accessed on 30 July 2020).
64. ESRI. *Arcgis Desktop: Release 10, Technical Report*; Environmental Systems Research Institute (ESRI): Redlands, CA, USA, 2010.
65. Storey, J.; Scaramuzza, P.; Schmidt, G. Landsat 7 scan line corrector-off gap filled product development. In Proceedings of the PECORA 16 Conference Proceedings, Sioux Falls, SD, USA, 23–27 October 2005.
66. Jaafar, H.H.; Ahmad, F.A. Time series trends of Landsat-based ET using automated calibration in METRIC and SEBAL: The Bekaa Valley, Lebanon. *Remote Sens. Environ.* **2020**, *238*, 111034. [[CrossRef](#)]
67. Lu, G.Y.; Wong, D.W. An adaptive inverse-distance weighting spatial interpolation technique. *Comput. Geosci.* **2008**, *34*, 1044–1055. [[CrossRef](#)]
68. Jing, M.; Wu, J. Fast image interpolation using directional inverse distance weighting for real-time applications. *Opt. Commun.* **2013**, *286*, 111–116. [[CrossRef](#)]
69. Doorenbos, J.; Kassam, A.H. *Yield Response to Water*; Volume FAO Irrigation and Drainage Paper No. 33; Food and Agriculture Organization of the United Nations (FAO): Rome, Italy, 1979.

70. FAO. *Maize in Human Nutrition*; United Nations Food and Agriculture Organization (FAO): Rome, Italy, 1992.
71. Lang, J. *Notes of a Potato Watcher*; Texas A&M University Press: College Station, TX, USA, 2001; p. 388.
72. Nitchou, M.; Midékor, A.; Sawadogo, B. *Restitution des Travaux de Suivi de la Campagne Saison Sèche 2014 Sur le Périmètre Rizicole de la Vallée du Kou*; AEDE/OE: Bobo-Dioulasso, Burkina Faso, 2014.
73. Javadian, M.; Behrangi, A.; Gholizadeh, M.; Tajrishy, M. METRIC and WaPOR Estimates of Evapotranspiration over the Lake Urmia Basin: Comparative Analysis and Composite Assessment. *Water* **2019**, *11*, 1647. [[CrossRef](#)]
74. Zwart, S.J.; Bastiaanssen, W.G.M. Review of measured crop water productivity values for irrigated wheat, rice, cotton and maize. *Agric. Water Manag.* **2004**, *69*, 115–133. [[CrossRef](#)]
75. Dembélé, Y.; Kambiré, H.; Sié, M. Gestion de l'eau et de l'azote en riziculture irriguée au Burkina Faso. *Cah. Agric.* **2005**, *14*, 569–572.
76. Unkovich, M.; Baldock, J.; Forbes, M. Chapter 5—Variability in Harvest Index of Grain Crops and Potential Significance for Carbon Accounting: Examples from Australian Agriculture. In *Advances in Agronomy*; Academic Press: Cambridge, MA, USA, 2010; Volume 105, pp. 173–219.
77. Dawe, D. Increasing Water Productivity in Rice-Based Systems in Asia—Past Trends, Current Problems, and Future Prospects. *Plant Prod. Sci.* **2005**, *8*, 221–230. [[CrossRef](#)]
78. Zwart, S.J. 21 Assessing and Improving Water Productivity of Irrigated Rice Systems in Africa. In *Realizing Africa's Rice Promise*; Wopereis, M.C.S., Johnson, D.E., Ahmadi, N., Tollens, E., Jollah, A., Eds.; CAB International: Wallingford, UK, 2013; p. 265.
79. Bos, M.G.; Abdel-Dayem, S.; Bastiaanssen, W.G.M.; Vidal, A. Remote sensing for water management: The drainage component. In *Proceedings of the World Bank Expert Consultation, organized by ICID, IPTRID, International Institute for Land Reclamation and Improvement (ILRI), and WaterWatch, Ede-Wageningen, The Netherlands, 15–16 May 2001*.



© 2020 by the authors. Licensee MDPI, Basel, Switzerland. This article is an open access article distributed under the terms and conditions of the Creative Commons Attribution (CC BY) license (<http://creativecommons.org/licenses/by/4.0/>).